6   Chapter Six: Applications

The validated methods described above were used to examine the influence of several process parameters on the glycosylation of the two model proteins. Special features of ProBioGen's products and services were used in order to find the relevant parameters for examination. These corresponded to the hollow fibre bioreactor system as specific production system and the continuous long-time cultivation of the CHO-cells, as well as the design and development of cell lines. Regarding the hollow fibre bioreactor system, it was interesting to examine the influence of the high cell density in the hollow fibre cartridges compared to other production systems such as SuperSpinners. Examining continuous cultivation, the effect of the long production time compared to batch- or fed-batch cultivation was the crucial point. Within cell line development, the selection of the best clone is the general goal. Today, the most important parameter for a good clone is its productivity. In this study, it should be investigated if the glycosylation potential of the selected clone could also be used as selection parameter. Due to the fact that multiple determinations of the same sample were not possible because of limited resources, variability of the analytical methods was estimated for each sample using the validation data in chapter 5. Standard deviations could be calculated by the following formula [163]

$$s^2 = \frac{\chi^2_{n-1;1-\alpha/2}}{n-1} \times \sigma^2$$

and therefore observed differences could be divided in significant and non-significant ones.

6.1   The influence of long-time cultivation in HFBR on the glycosylation pattern of a CHO-expressed monoclonal antibody

In this study, the influence of hollow fibre bioreactor production parameters

on the glycosylation pattern of CHO-Mab was studied. Therefore two different production processes were performed. The first production process was in small scale using an ASM-bioreactor to establish a stable production process. After that, the process was upscaled to an ASX-bioreactor. Cell age seemed to have an influence on the glycosylation pattern of CHO-Mab.

6.1.1 CHO-Mab-ASM-process

CHO-Mab was cultivated in the ASM containing two hollow fibre cartridges over a period of 63 days. Harvest bulks were continuously examined during the process. The intra-batch-consistency of the harvested product bulks was investigated.

6.1.1.1 Oligosaccharide identification of CHO-Mab (ASM)

MALDI-TOF-MS of CHO-Mab produced in the ASM resulted in four peaks with the following structures: (HM=1378, G0F=1606, G1F=1768, G2F=1930) (Figure 39 + 40). All harvest bulks showed qualitative identical MS-spectra.
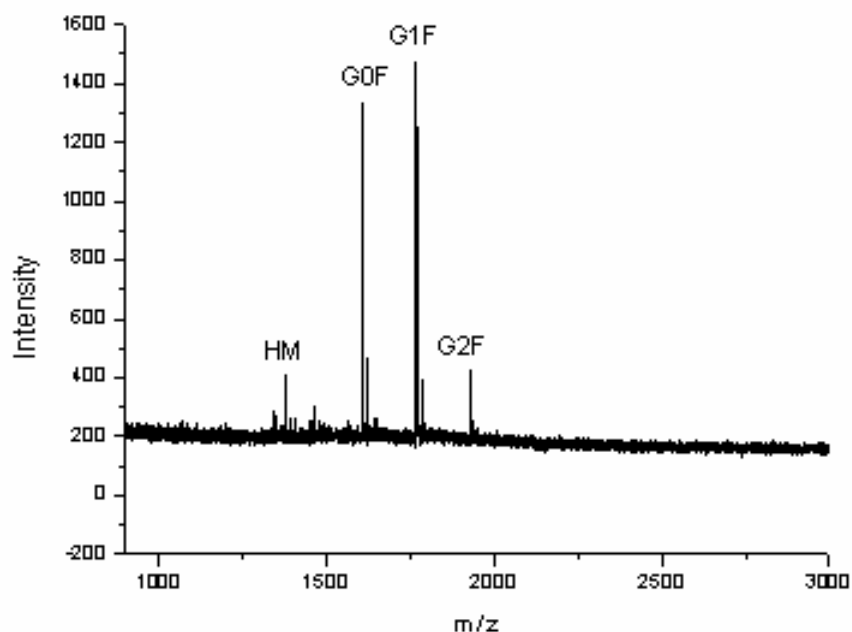

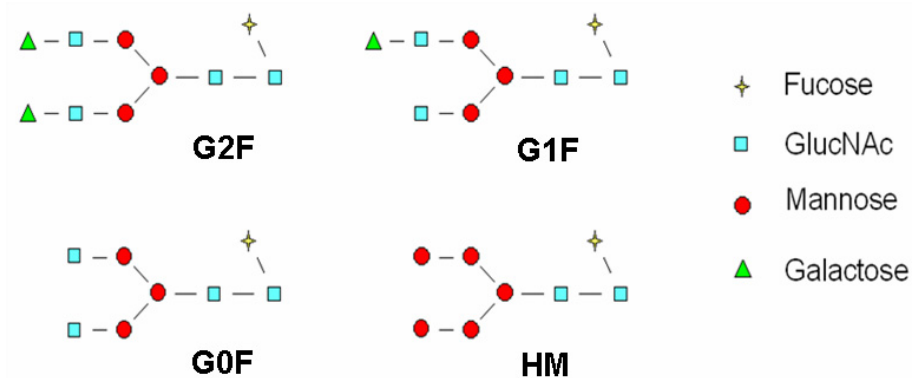Figure 39: MALDI-TOF-MS-structure identification for CHO-Mab-ASM

Figure 40: Identified N-glycans of CHO-Mab

6.1.1.2 Measured process parameters

As production parameters productivity, product amount, dissolved oxygen (DO) and cell removal rate were measured (Figure 41 - 44). Because of the fact that the hollow fibre bioreactor was a closed system, the amount and vitality of the cells could not be measured. Therefore productivity was calculated in product amount per hollow fibre cartridge and time and not as usual in product amount per defined amount of cells and time. For the vitality of the cells the DO was used as surrogate parameter. The process was characterized by a very slow growth phase of the cells with an increasing productivity up to day 40. This correlated with a slowly increasing oxygen consume. Only an extensive cell removal of old and dead cells from day 42 - 53 led to an acceleration in cell-growth and finally the stationary phase was reached. DO reached a minimum (Figure 42). At day 63 the process was stopped. In the end, one gram of CHO-Mab was produced (Figure 44).
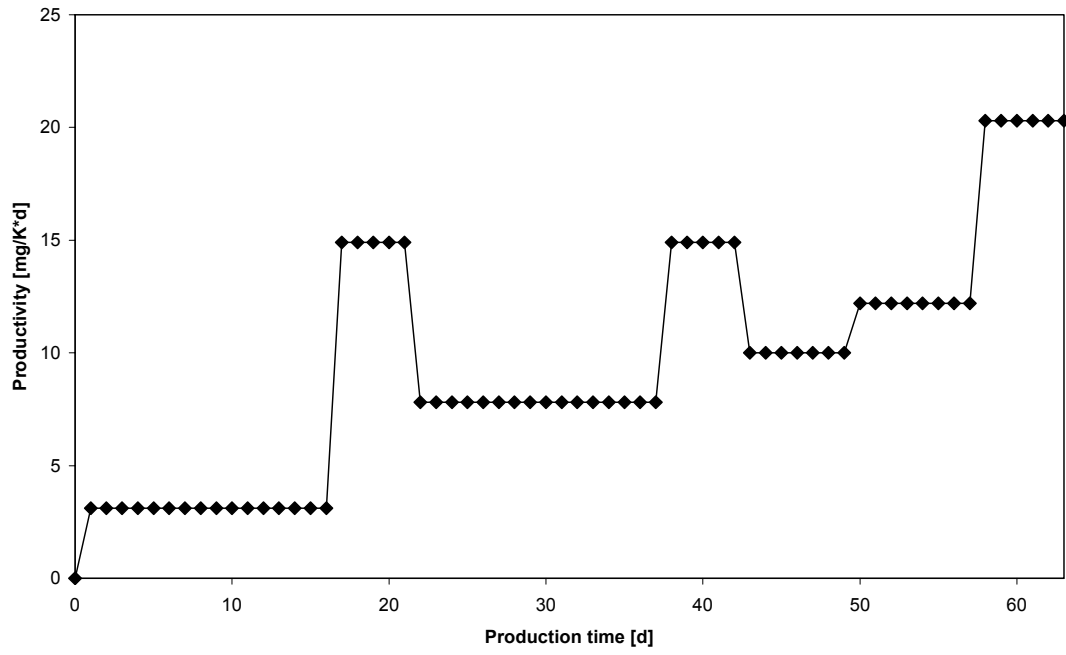
178

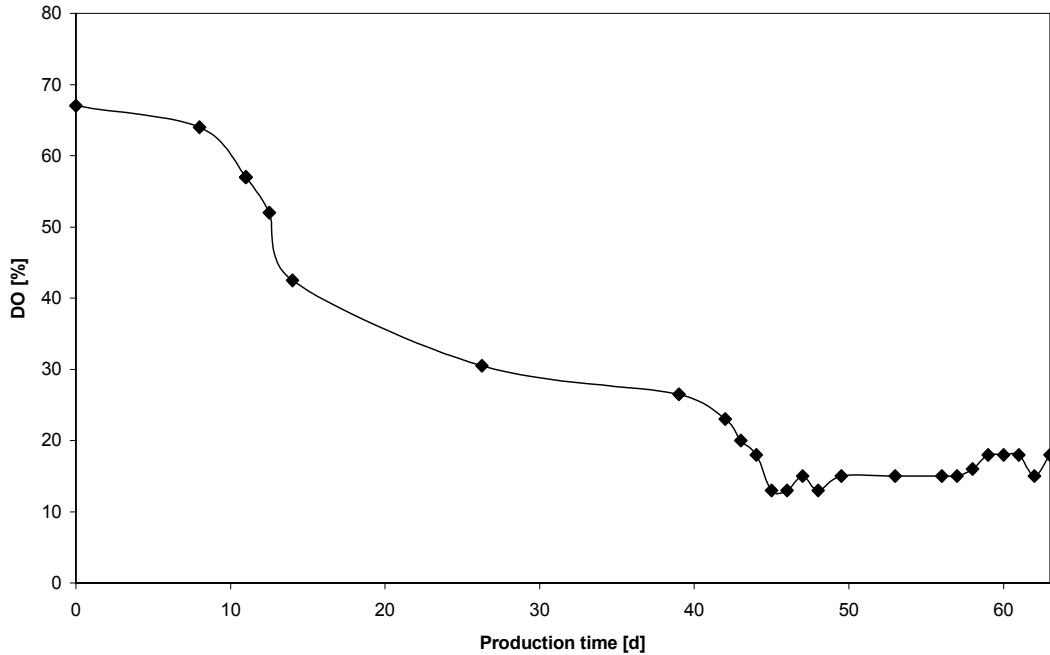Figure 41: CHO-Mab-productivity during the ASM-process

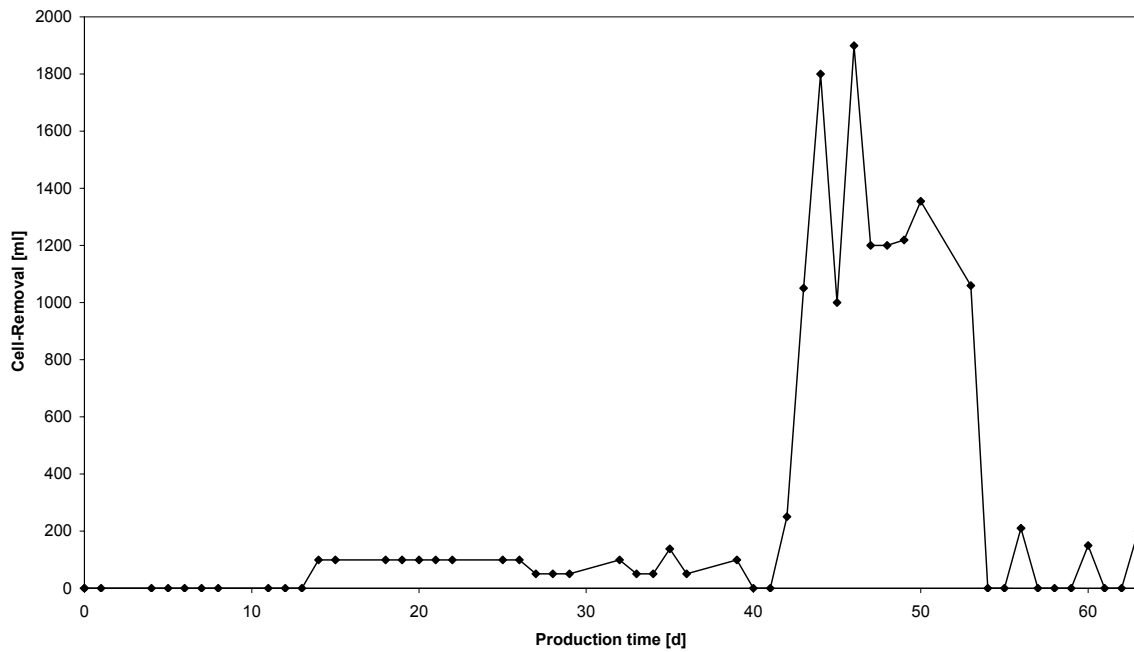

Figure 42: DO-curve during the CHO-Mab-ASM-process
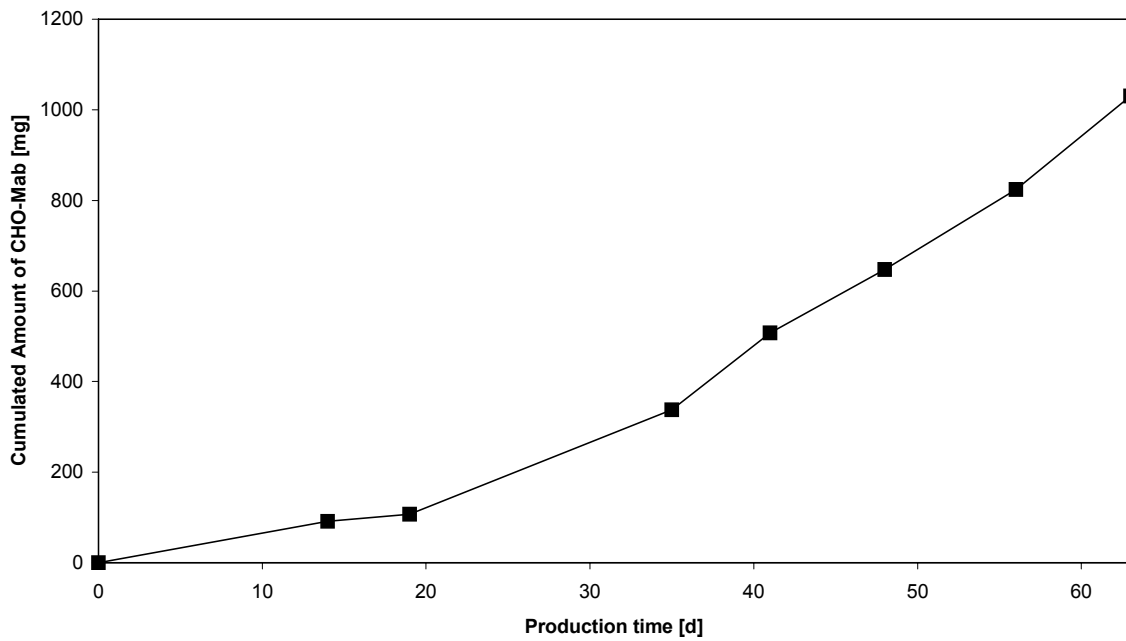
Figure 43: CHO-Mab-ASM-process - Cell removal

Figure 44: Cumulated amount of CHO-Mab during the ASM-process

180

6.1.1.3 Quantitative glycosylation analysis

Sialylation rate (GlycoSepC-HPLC):

All samples showed similar chromatograms with three defined peaks, first an A0-fraction (no sialic acid; $A0_{average}$ = 86.0±1.0%), second an A1-fraction (one sialic acid; $A1_{average}$ = 5.8 ±1.0%) and third an A2-fraction (two sialic acids; $A2_{average}$ = 8.2±1.0%). Sialylation patterns stayed nearly consistent during the whole process. The major part of the structures belonged to the A0-fraction and minor parts to A1 and A2 (Figure 45), except for the period from day 0 - 15 and the period from day 41 - 48. From day 0 - 15, A0 was higher and A2 lower than in the rest of the process and from day 41 - 48, sialylation rate increased with a reduced A0- and a doubled A2-fraction in correlation with an extensive cell removal procedure.
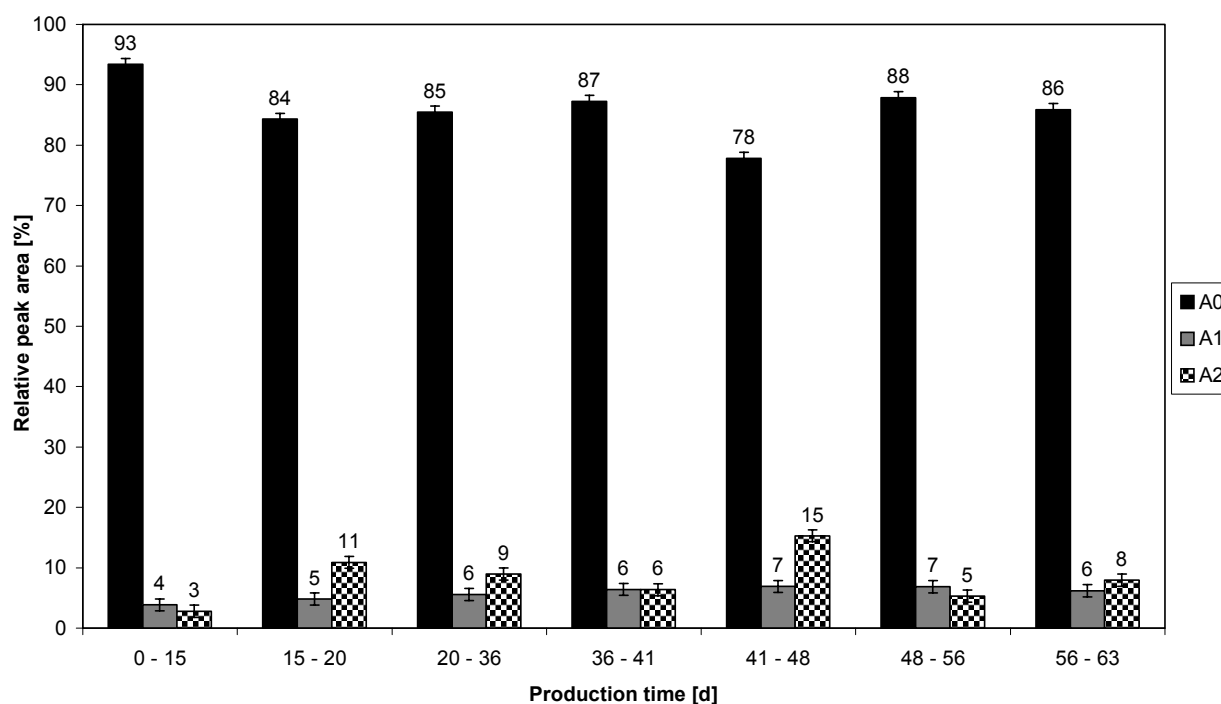

Figure 45: CHO-Mab-ASM-process - sialylation rate[26]

---

[26] Error bars: $VK_{n=2} = \sqrt{VK^2_{n->\infty} \times \chi^2_{1/0.975}} = 1.0\%$ with $VK^2_{n->\infty} = \dfrac{VK^2_{n=4}(Table\,26)}{\chi^2_{3/0.975}} \times 3$

Galactosylation rate (Aminophase-HPLC):

The aminophase chromatograms showed also nearly consistent patterns for the different samples (Figure 46). Four major peaks were identified: $HM_{average}$ (10.0±3.2%), $G0F_{average}$ (26.4±3.2%), $G1F_{average}$ (46.0±3.2%) and $G2F_{average}$ (17.6±3.2%). In correspondence to the GlycoSepC-results, the first harvest bulk up to day 15 showed less G2F- and higher G0F-structures. Due to the missing galactose-residues, G0F-structures could not be sialylated. Also in correspondence to the GlycoSepC-results, the harvest bulk of day 41 - 48 showed less G0F- and higher G2F-structures which were predestined to be higher sialylated.
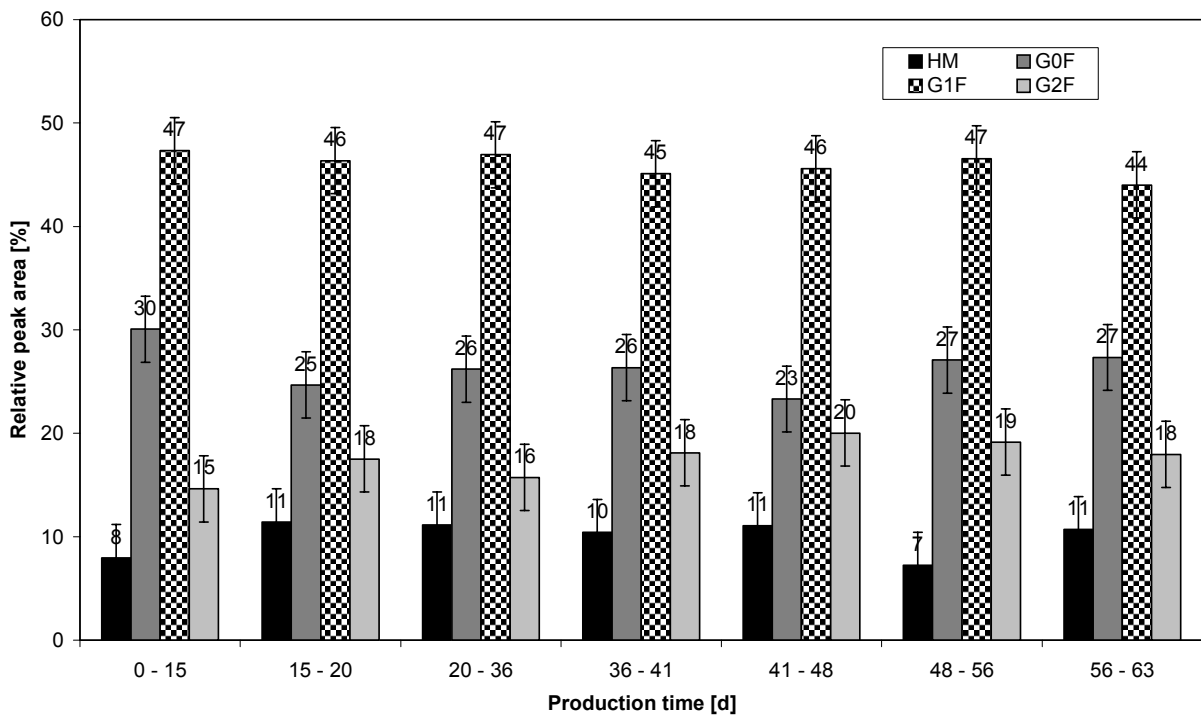

Figure 46: CHO-Mab-ASM-process - AP-patterns[27]

---

[27] Error bars: $VK_{n=2} = \sqrt{VK_{n\to\infty}^2 \times \chi_{1/0.975}^2} = 3.2\%$ with $VK_{n\to\infty}^2 = \dfrac{VK_{n=4}^2 (Table\,28)}{\chi_{3/0.975}^2} \times 3$

6.1.1.4 Conclusions

Due to the long growth phase of the cells with a corresponding increasing productivity, an observation of the influence of cultivation time was nearly not possible. The cells did only reach a steady state production phase between day 45 and 60. This period of 15 days was too short to observe any trends in glycosylation. The process was characterized by process variations which probably led to the observed minor changes in glycosylation. In general, the ASM-process could be used to get to know the crucial points of the CHO-Mab-process including cell behavior, pump settings of the bioreactor, etc. to optimize the later production of CHO-Mab in the ASX-bioreactor.

6.1.2 CHO-Mab-ASX-process

Because of the knowledge of the ASM-production process, CHO-Mab could be cultivated over a period of 82 days in a continuous production process in an ACUSYST X-CELL bioreactor containing six hollow fibre cartridges. Harvest bulks were also examined continuously during the process. This time, the aim was to bring the cells quickly into a steady state production phase and to run this steady state phase as long as possible to examine the influence of the long-time cultivation on the glycosylation of CHO-Mab.

6.1.2.1 Oligosaccharide identification of CHO-Mab (ASX)

MALDI-TOF-MS of CHO-Mab produced in the ASX identified also the four structures detected in the ASM-process (HM=1378, G0F=1606, G1F=1768, G2F=1930) (Figure 47). All harvest bulks showed qualitative identical MS-spectra.
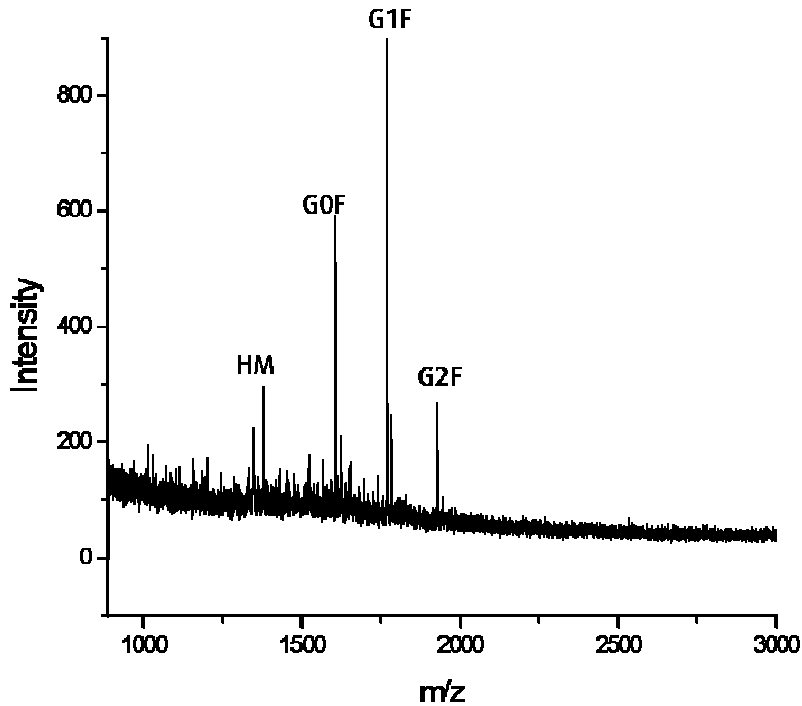
Figure 47: CHO-Mab-ASX-process - MALDI-TOF-MS for structure identification

6.1.2.2 Measured process parameters

Post inoculation the cells grew exponentially in the bioreactor system and steady state was reached at day 25, characterized by a nearly consistent productivity of the cells (Figure 48). DO in the nutrition medium (Figure 49) changed according to the growth rate of the cells. Due to the experience made in the ASM-process, the cell removal was more effective. After a steady state phase of 50 days, the influence of a new nutrition medium should be investigated. At day 74, the nutrition medium was changed from ProCHO4-CDM (Cambrex) to PBG 1.0 medium (Hyclone). The consequence was a dramatic cell death visible by a strong decrease in productivity and an increase in DO. The cells were not able to handle the stress of the medium change in this short period of time. At the end of the process 8.5 g CHO-Mab were produced. On day 63, 6 g CHO-Mab were produced. This were six times more than in the ASM-process (Figure 50) by an only three times higher culture volume (6 HFBR-cartridges in the ASX vs. 2 HFBR-cartridges

in the ASM). So effectively, productivity doubled in the ASX due to improved processing.
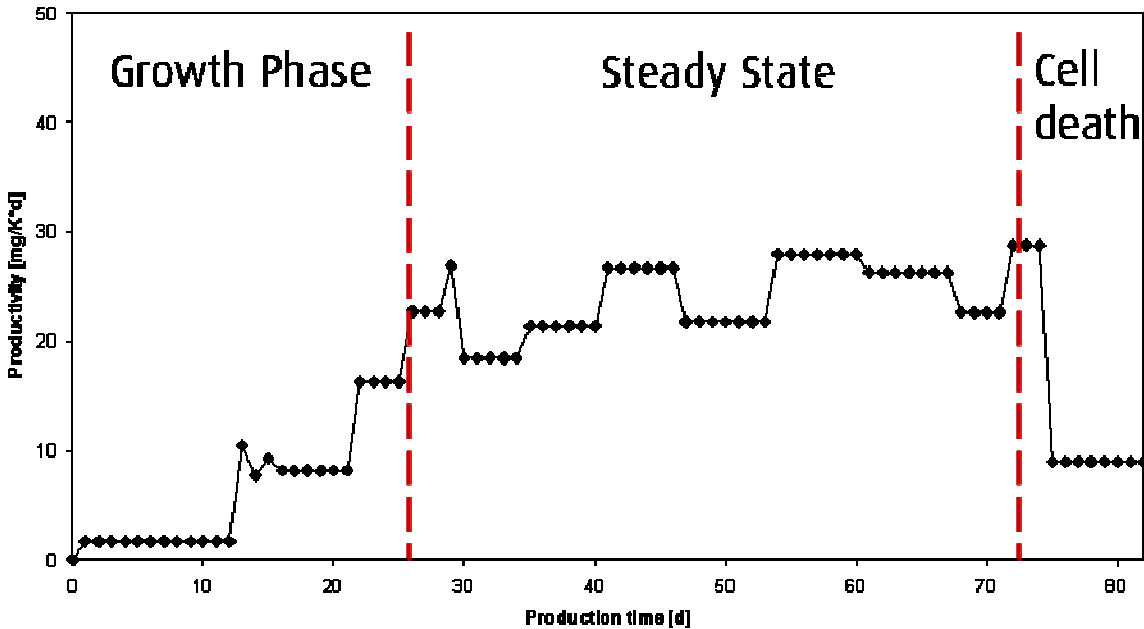

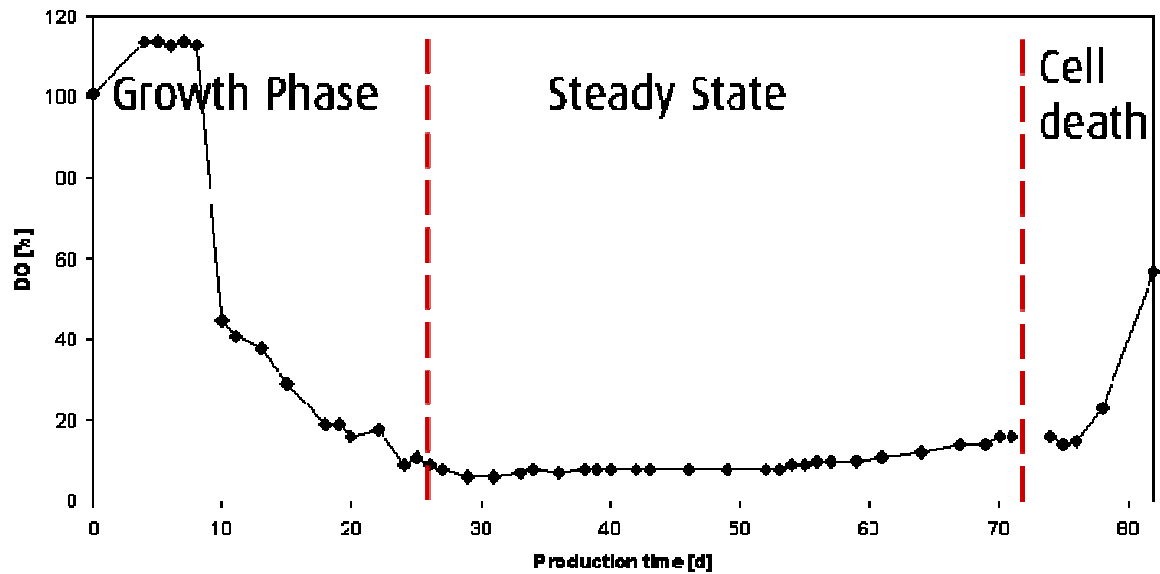Figure 48: CHO-Mab-productivity during ASX-process

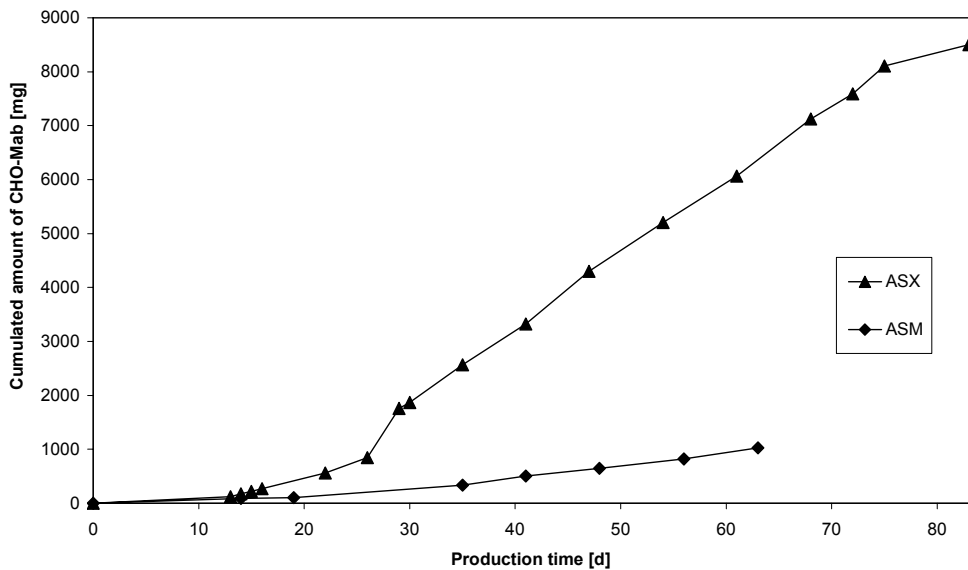Figure 49: CHO-Mab-ASX-process - measurement of dissolved oxygen (DO)

Figure 50: Cumulated amount of CHO-Mab during the ASX-production process and comparison with the ASM-process *(ASX = 6 HFBR-, ASM = 2 HFBR-cartridges)*

6.1.2.3 Quantitative glycosylation analysis

Sialylation rate (GlycoSepC-analysis):

All samples showed similiar chromatograms with three defined peaks, first an A0-fraction (no sialic acid; $A0_{average}$ = 89.4±1.0%), second an A1-fraction (one sialic acid; $A1_{average}$ = 5.0±1.0%) and third an A2-fraction (two sialic acids; $A2_{average}$ = 5.6±1.0%) (Figure 51). Sialylation rates were consistent and as expected from the ASM-process very low over the whole production process.
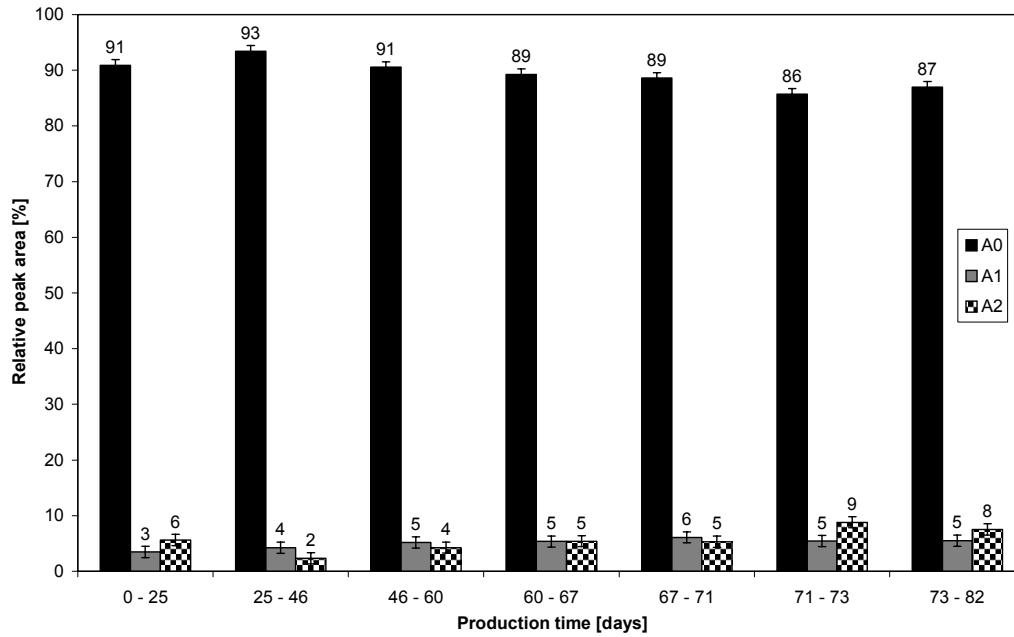
Figure 51: CHO-Mab-ASX-process - Level of sialylation[28]

Galactosylation rate (Aminophase-analysis):

The aminophase chromatograms showed also qualitative consistent patterns for the different samples. Four major peaks were identified: $HM_{average}$ ($12.1\pm3.2\%$), $G0F_{average}$ ($27.9\pm3.2\%$), $G1F_{average}$ ($44.4\pm3.2\%$) and $G2F_{average}$ ($15.7\pm3.2\%$) (Figure 52). Two significant trends in the glycosylation pattern could be observed. The galactosylated structure G1F decreased significant, therefore the preprocessed structure HM increased (Table 41).

---

[28] Error bars: $VK_{n=2} = \sqrt{VK_{n->\infty}^2 \times \chi_{1/0.975}^2} = 1.0\%$ *with* $VK_{n->\infty}^2 = \dfrac{VK_{n=4}^2 (Table\,26)}{\chi_{3/0.975}^2} \times 3$
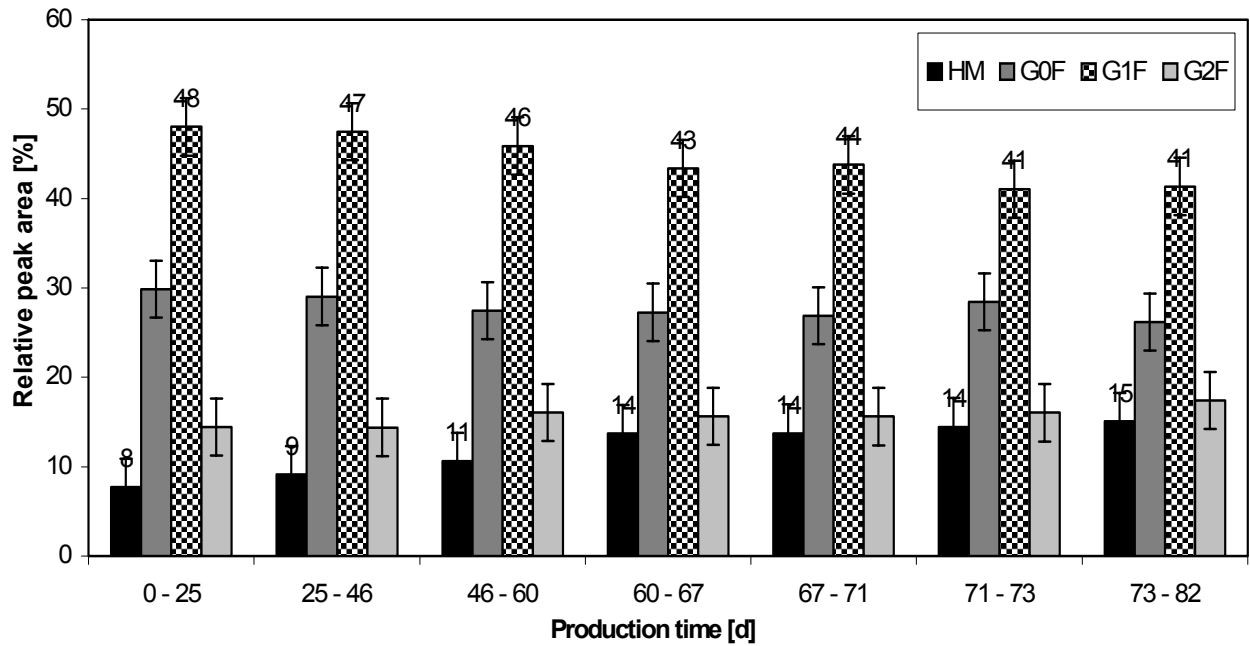
Figure 52: CHO-Mab-ASX-process - Level of galactosylation[29]

Table 41: Decrease of higher antennary complex (G1F) and increase of preprocessed (HM) structures during the CHO-Mab-ASX-process

Batch Structure	Day 0 - 25	Day 73 - 82
HM	8%	15%
G1F	48%	41%

6.1.2.4 Conclusions

In contrast to the CHO-Mab-ASM-process, the ASX-process was characterized by a quick growth phase of the cells and a resulting higher productivity. A steady state production phase of 50 days was reached and trends in glycosylation became obvious. During the steay state phase, the

---

[29] Error bars: $VK_{n=2} = \sqrt{VK^2_{n->\infty} \times \chi^2_{1/0.975}} = 3.2\%$ $\ with\ VK^2_{n->\infty} = \dfrac{VK^2_{n=4}(Table\,28)}{\chi^2_{3/0.975}} \times 3$

complexity of the glycan structures decreased regarding antennarity and a shift from G1F- to HM-structures could be observed, possibly due to an aging process of the cell-internal glycosylation machinery. Preprocessed structures like HM were not further synthesized to complex structures, maybe due to a developing inability of several glycosyltransferases at longer cultivation times. The sialylation rate of CHO-Mab was too low to react significant on this change, so that no trend in sialylation was noted.

Continuous production processes often miss the possibility to get stopped at the right time. Alternative end-points for these processes could be predefined limits of several crucial glycan structures, such as HM [164].

6.2 Finding the right clone - a cost-saving and efficient strategy

Today, productivity is considered as the main parameter for clone selection. This study should show that glycosylation can be an essential factor in the clone selection procedure. Although specific activity reflects product integrity, the degree of glycosylation is a major determinant of pharmacokinetic properties. Therefore, it has to be taken into account when a final producer clone is selected. An integrated approach is required to generate several highly productive clones and to evaluate them in the shortest time frame possible.

6.2.1 Clone creation

Clones 2, 3 and 4 were used for this study. They were created by RMCE of a functionalized cell line as described in Chapter 3.2.2 (Figure 53 + Figure 54).
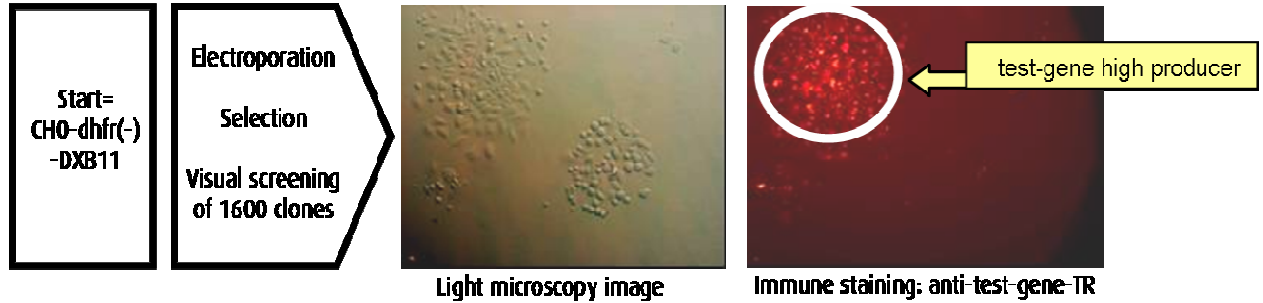

Figure 53: Identification of high producers of the test gene product using immunoprecipitation (TR = test reaction)
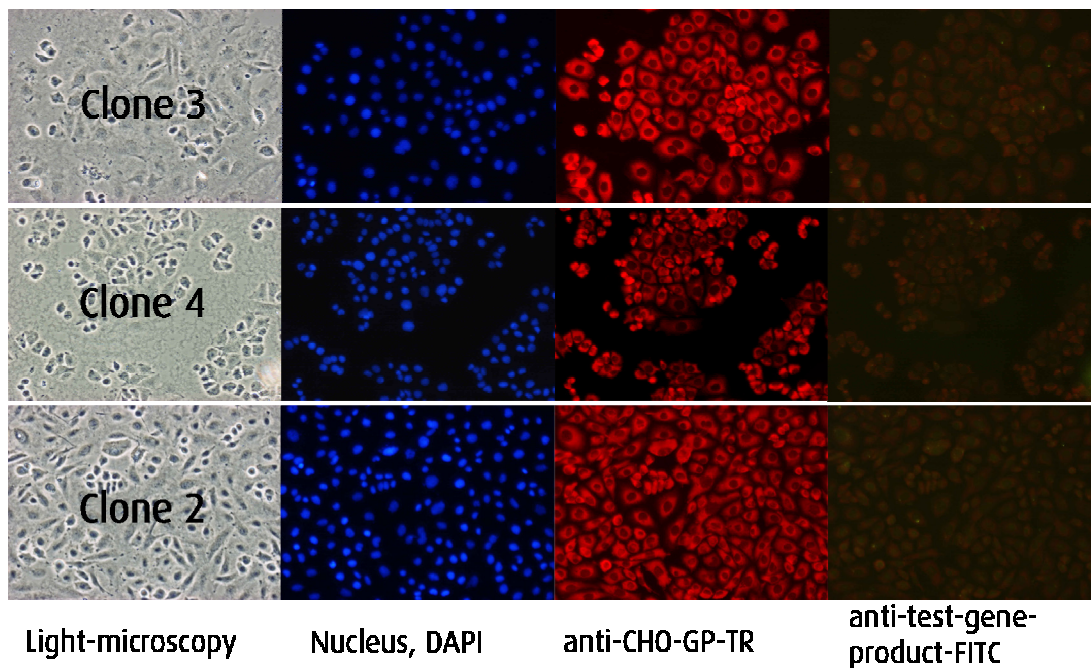

Figure 54: Immunofluorescent staining demonstrated the absence of the test gene (green) and the homogeneous expression of the target gene (red) (TR = test reaction, FITC = fluorescein isothiocyanate)

6.2.2 Productivity

Productivity of the clones was measured in a 24h-productivity-assay (Table 42). The assay was performed in 12-well-plates with 1 ml culture volume per well. At first, the cells were multiplied up to a sufficient cell amount of 1 x 10^5 cells per clone per well with a minimal vitality of 70%.

Cell counting and vitality determination of the cells was performed using the ViCell Cell Viability Analyzer (Beckman Coulter) with a standardized operation procedure. The principle of this measurement laid in the coloration of dead cells by trypan blue and the count of the cells in a Neubauer-counting chamber.

For the productivity assay, the cells were cultivated in fresh nutrition medium over a period of 24 hours under defined incubator conditions. After 24 hours a determination of the produced CHO-GP was performed by a standardized ELISA.

The productivity of the cells could be calculated by the following formula:

$$Specific\ productivity = \frac{c_x * 10^6}{\Delta t * \dfrac{vCN * 100\%}{vitality}} \left[\frac{pg}{d * cell}\right]$$

$c_x = product\ concentration\ after\ 24\ hours\ [\mu g\,/\,ml]$
$\Delta t = time\ [d]$
$vCN = vital\ cell\ number\ [/\,ml]$
$vitality = vitality\ [\%]$

Table 42: Results of 24h-productivity-assay

Clone	Productivity [pg/d*cell]	Relative Productivity [%]
3	16	100
4	12	75
2	16	100

Clone 2 and 3 had a higher productivity than clone 4, but a further decision between them could not be made. Therefore activity of the produced CHO-GP of each of the three clones was compared.

6.2.3 Activity of CHO-GP

CHO-GP was tested in an in-vitro-assay (Table 43) which cannot be described more detailed because of intellectual property rights.

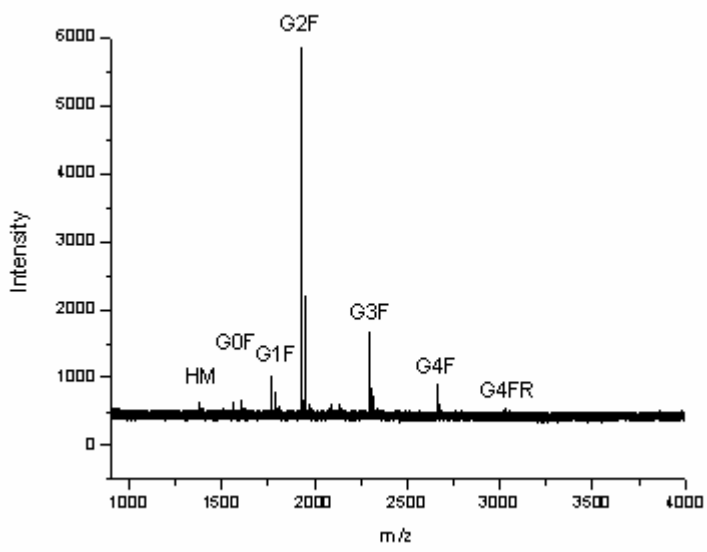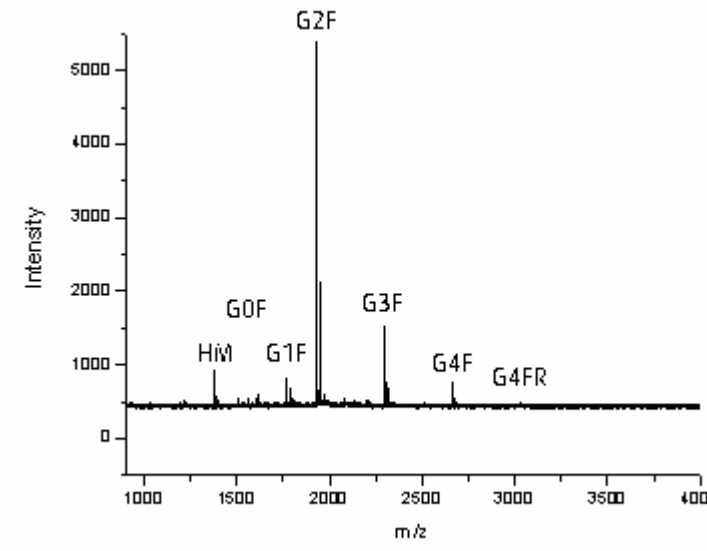Table 43: Results of activity assays of CHO-GP produced by the different clones

CHO-GP of clone	Activity [%]
3	75
4	100
2	75

As result, CHO-GP of clone 4 showed the highest activity of the three clones. Due to the fact that clone 4 was the least productive clone, differences compensated each other. Finally, glycosylation analysis of the produced CHO-GP was used as a third tool for the selection procedure.

6.2.4 Oligosaccharide identification of CHO-GP

MALDI-TOF-patterns of CHO-GP-N-glycans identified seven N-glycan-structures which could also be quantified by Aminophase-analysis (Table 44) (Figure 55).

Table 44: MALDI-TOF-MS-patterns of all three CHO-GP-variants

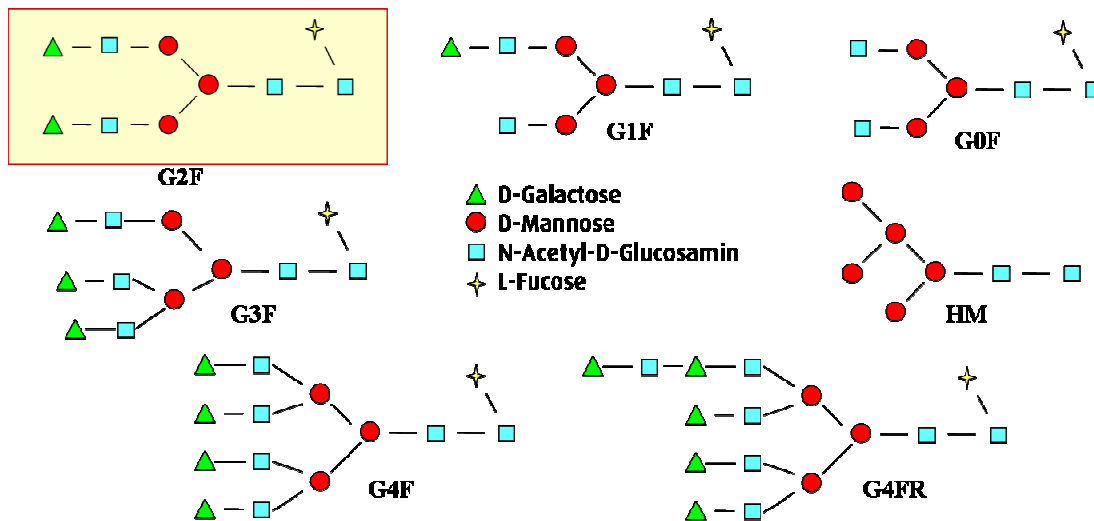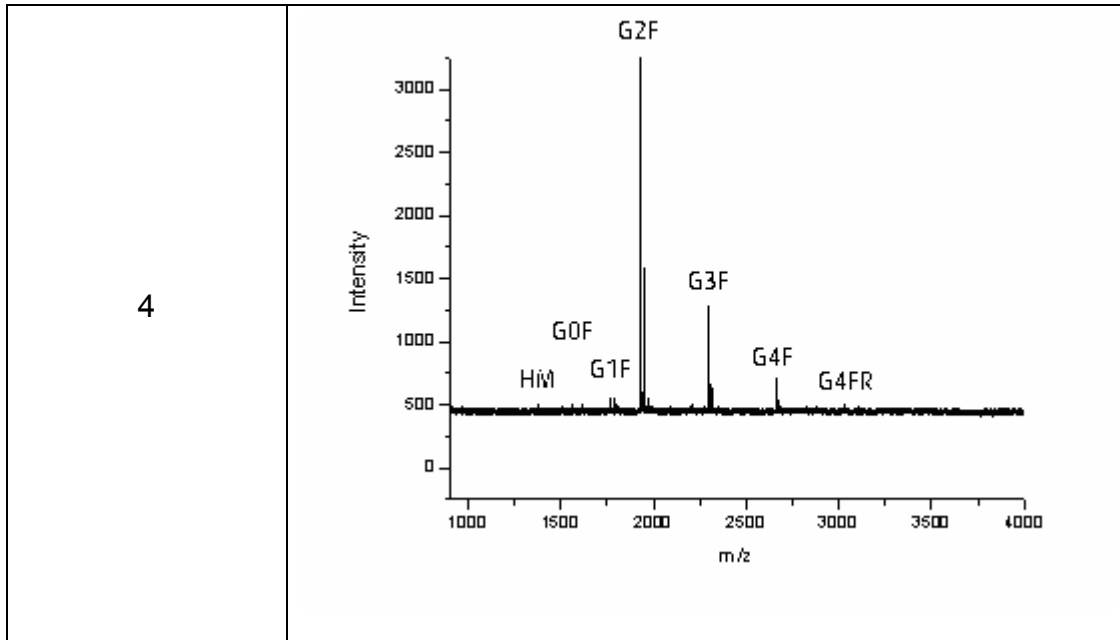| Clone	MALDI-TOF-MS-pattern
2	
3	

4	

Figure 55: Identified and quantifiable CHO-GP-N-glycans (yellow box = most common neutral structure of all CHO-GP-N-glycans)

6.2.5 Quantitative glycosylation analysis

Sialylation rate (GlycoSepC-analysis):

GlycoSepC-patterns of CHO-GP-samples of all clones showed five peaks (A0-A4). But the samples differed in their level of sialylation, especially in

their A0/A2-relation (Figure 56). The amount of A1-, A3- and A4-structures was nearly the same for all clones. The clones differed significant in their A0- and A2-structures where clone 2 had the lowest and clone 4 the highest A2/A0-ratio. So the level of A2 could be used as clone selection criterium. Because of the highest amount of bisialylated complex structures (A2) for clone 4, this clone was the best within this selection.
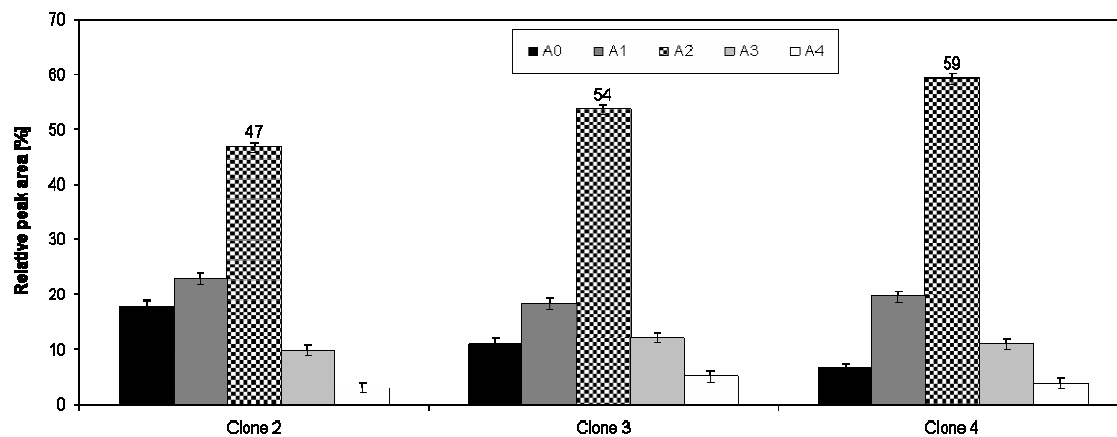

Figure 56: Distribution of sialylated structures of the different clones[30]

Galactosylation rate (Aminophase-analysis):

The Aminophase-analyses corresponded to the GlycoSepC-results (Figure 57). Clone 4 showed significant more neutral biantennary complex structures and less HM-, G0F- and G1F-structures than the other two clones. In CHO-cells, sialic acids are bound with their C-2 at the C-3 of the endstanding galactose-residues. Only galactosylated structures are able to bind a sialic acid. HM, G0F and G1F are not able to bind two sialic acids (A2). These structures were increased for clone 2 and 3. A very reasonable explanation ,why clone 4 showed the highest amount of A2-structures, was that it also had the highest amount of G2F-structures.

---

[30] Error bars: $VK_{n=2} = \sqrt{VK_{n->\infty}^2 \times \chi_{1/0.975}^2} = 1.0\%$ with $VK_{n->\infty}^2 = \dfrac{VK_{n=4}^2 (Table\,26)}{\chi_{3/0.975}^2} \times 3$
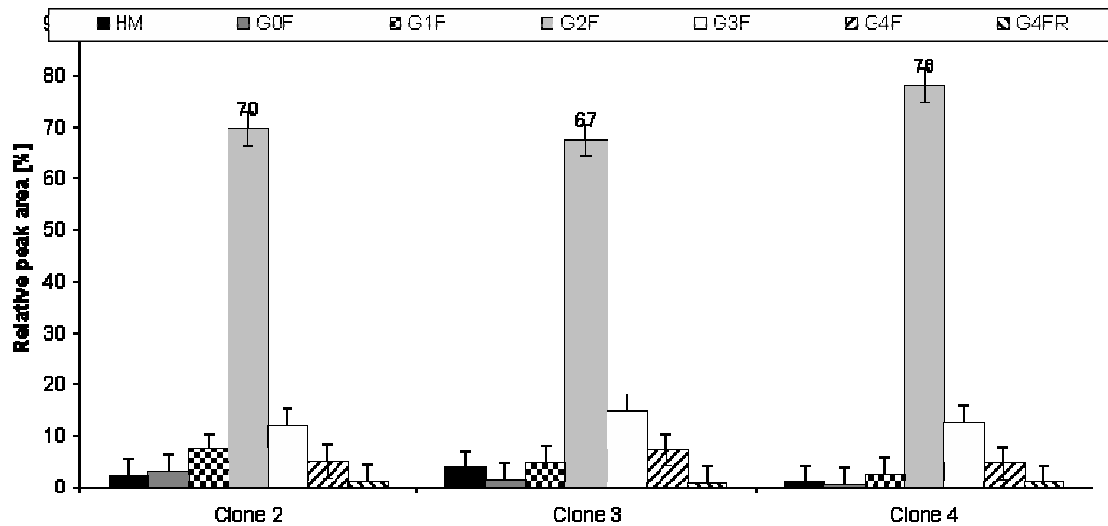
Figure 57: Distribution of neutral CHO-GP-glycans from different clones[31]

6.2.6 Conclusions

Productivity of the clones and activity of the produced CHO-GP by the clones compensated each other. Clone 4 was selected for production because CHO-GP from this clone had the highest amount of sialylated A2-structures and therefore probably better pharmacokinetic characteristics.

Only the combination of the selection criteria, productivity, activity and glycosylation led to the best choice of clone for therapeutic protein manufacturing (Figure 58).

	Productivity [%]	Activity [%]	Sialylation (A2) [%]
Clone 2	100	75	54
Clone 4	75	100	59
Clone 5	100	75	47

Figure 58: Final clone selection criteria

---

[31] Error bars: $VK_{n=2} = \sqrt{VK_{n->\infty}^2 \times \chi_{1/0.975}^2} = 3.2\%$ with $VK_{n->\infty}^2 = \dfrac{VK_{n=4}^2 (Table\,28)}{\chi_{3/0.975}^2} \times 3$

6.3 The influence of cell density on CHO-GP-glycosylation

A significant criterium for protein production in hollow fibre bioreactors is the high cell density of the producer cells. To examine if different cell densities in hollow fibre bioreactor systems have an influence on glycosylation, CHO-GP was produced by clone 1 in a SuperSpinner (low cell density) and in an ASM-bioreactor (high cell density). The production run in the SuperSpinner was performed in PBG 1.0 medium (Hyclone) over a period of 4 weeks. PBG 1.0 medium was a mixture of amino acids, glucose and salts that was optimally designed for clone 1. To be able to compare the continuous production in the ASM with the batch-production in the SuperSpinner, a continuous process design for the SuperSpinner was simulated. Therefore a repeated medium change combined with a harvest procedure was performed during the process. The harvest of the medium change on day 19 was purified and the purified sample was analyzed. The production run in the ASM was also performed in PBG 1.0 medium (Hyclone) over a period of 90 days. The first harvest bulk was examined after the cells had reached the steady state phase (day 20) and was compared with the SuperSpinner-sample.

6.3.1 Measured process parameters

The cell densities in the SuperSpinner could be measured directly by taking aliquots at different times over the process and using the ViCell Cell Viability Analyzer (Beckman Coulter) for cell counting. The average cell density during the process was calculated by taking the arithmetic average of all single cell densities (Figure 59). The average cell density of all cells was calculated to be $1.4*10^6$ cells/ml and the average cell density of the vital cells was $1.1*10^6$ cells/ml. The cell density of the SuperSpinner-harvest bulk was around $1*10^6$ cells/ml.
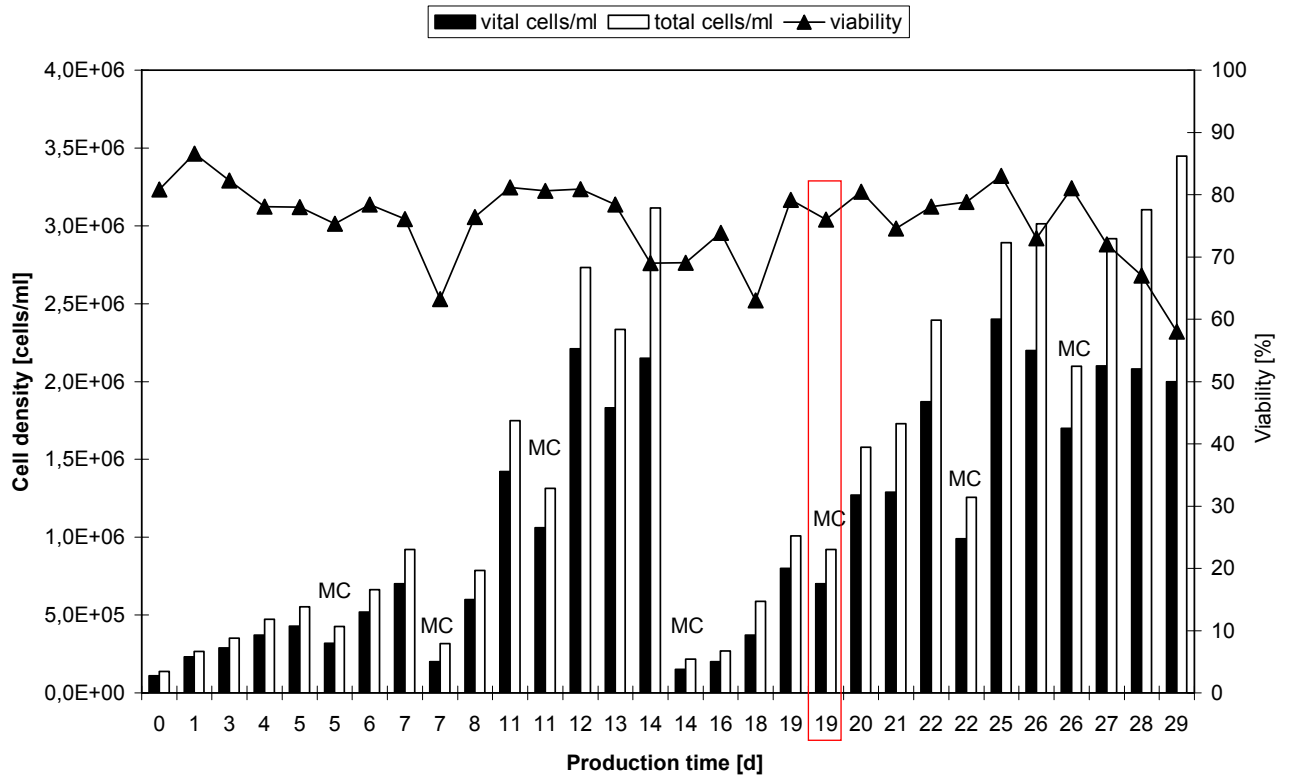
Figure 59: Cell density in the CHO-GP-SuperSpinner-process[32]

For the CHO-GP-ASM-process DO and productivity of the cells were measured (Figure 60). When cell growth reached the steady state phase, characterized by a plateau of the DO-curve and by a maximum productivity, the harvest bulk for glycosylation analysis was taken. The continued process was characterized by a slowly decreasing productivity. Another reason for the examination of the harvest bulk from day 20 was that SuperSpinner- and ASM-samples should be comparable in cultivation times. Later ASM-samples were also not taken into account because the effects of cell aging described in chapter 6.1 should not influence the effects of cell density on glycosylation.

Because of the fact that the hollow fibre cartridge was a closed system, no direct cell density measurements could be performed. Therefore cell density was calculated by a theoretical model. By macroscopic examination, the hollow fibre cartridge has become overgrown at day 20 (Figure 61).

---

[32] *MC = Medium Change; Strong decreases in cell densities after medium changes were due to the action of transferring cells out of the SuperSpinner during the MC; Red quarter = harvest bulk taken for glycosylation analysis*

Assuming a theoretical volume per cell of 2 pl, then $5*10^8$ cells would replace 1 ml at most packing density. One hollow fibre cartridge contained 100 ml, so that a maximum number of $5*10^{10}$ cells would be theoretically able to fill out one cartridge. To get a well handable, more realistic value for comparison with the SuperSpinner, a cell density of $1*10^8$ cells/ml was estimated for the ASM-bioreactor.
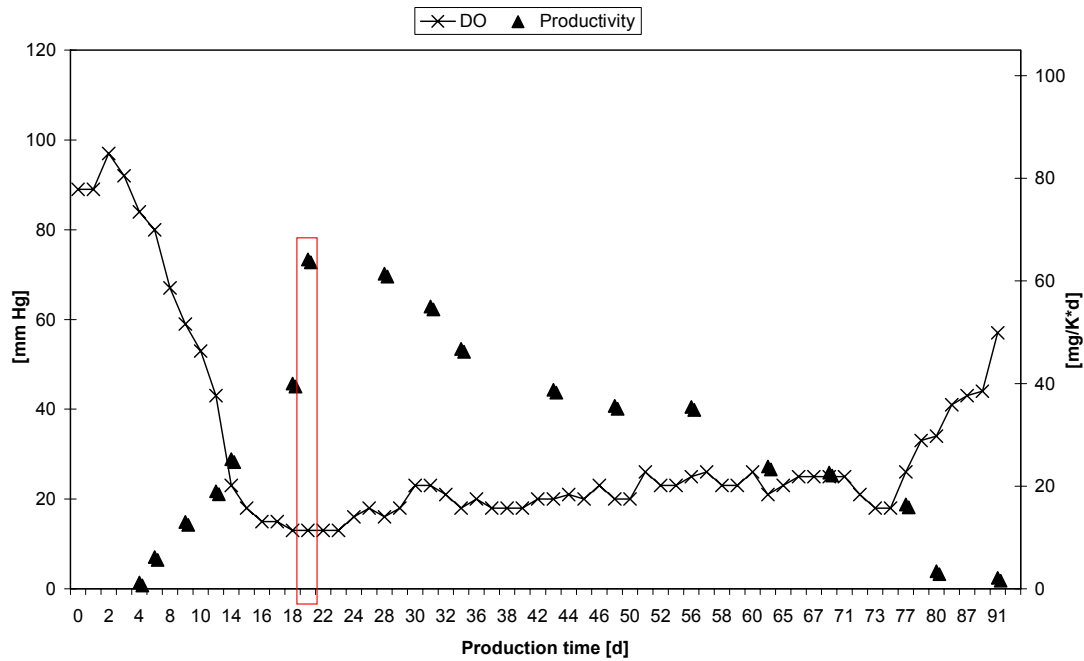
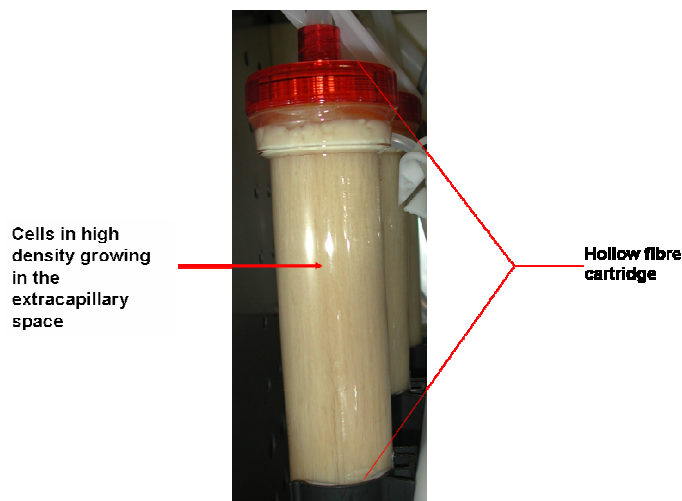Figure 60: DO and productivity in the CHO-GP-ASM-process[33]

Figure 61: Hollow fibre cartridge at day 20 of the CHO-GP-ASM-process

---

[33] *Red quarter = harvest bulk taken for glycosylation analysis*

As result, the cell density in the ACUSYST MAXIMIZER was estimated to be 100 times higher than in the SuperSpinner.

6.3.2 Oligosaccharide identification (MALDI-TOF-MS)

MALDI-TOF-MS of the two samples showed the characteristic structures of CHO-GP indicating qualitative identity (Table 45).

Table 45: MALDI-TOF-spectra of CHO-GP from different cell densities[34]

Bioreactor	MALDI-TOF-MS-pattern
ASM	
SuperSpinner	

---

[34] *SuperSpinner = low cell density, ASM = high cell density*

6.3.3 Quantitative glycosylation analysis

Sialylation rate (GlycoSepC-analysis):

Both samples showed similiar chromatograms with five defined peaks (A0 - A4). CHO-GP produced by the SuperSpinner and the ASM showed very similiar patterns, independent of the differences in cell density (Figure 62).
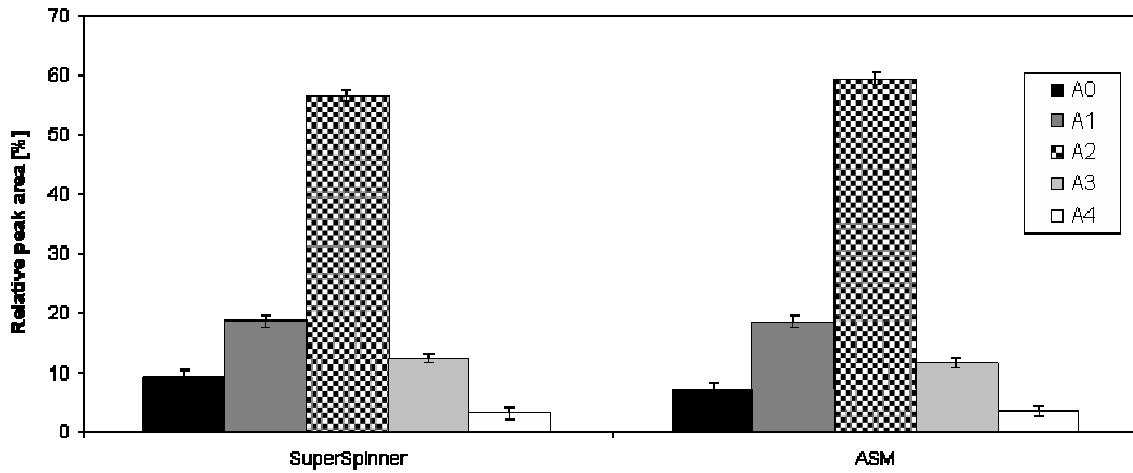

Figure 62: CHO-GP-sialylation in two hollow fibre production systems with different cell densities[35]

---

[35] *SuperSpinner = low cell density, ASM = high cell density;* Error

bars: $VK_{n=2} = \sqrt{VK^2_{n->\infty} \times \chi^2_{1/0.975}} = 1.0\%$ *with* $VK^2_{n->\infty} = \dfrac{VK^2_{n=4}(Table\,26)}{\chi^2_{3/0.975}} \times 3$

Galactosylation rate (Aminophase-analysis):

Both samples showed very similar aminophase chromatograms, qualitative as well as quantitative (Figure 63).
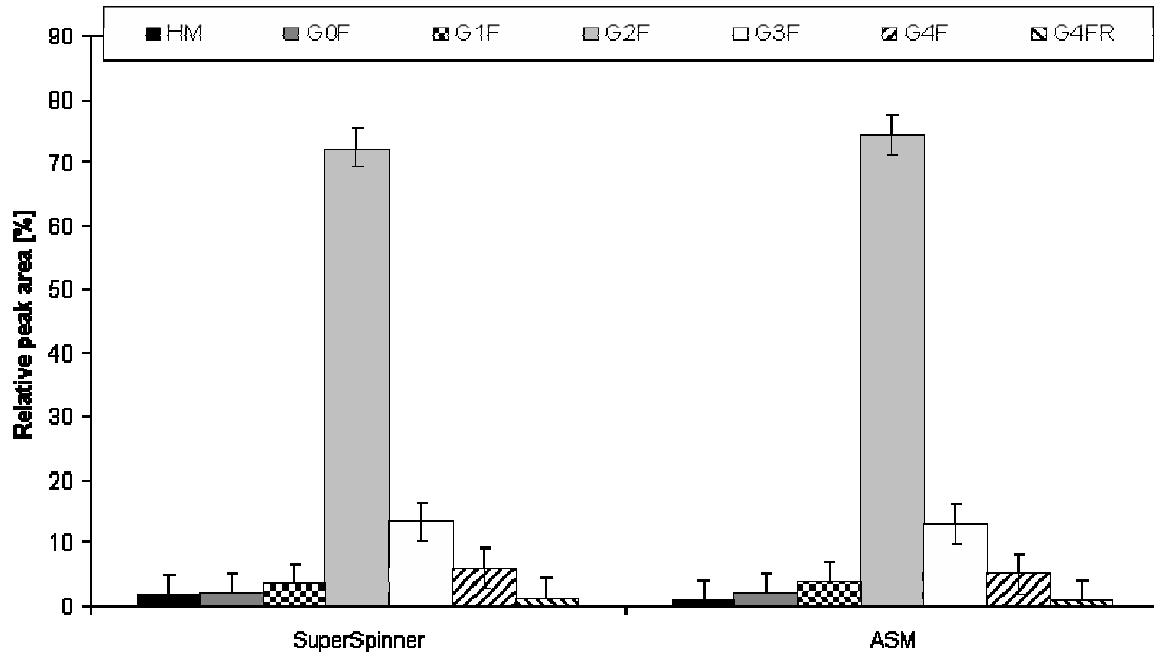

Figure 63: Distribution of neutral glycan structures of CHO-GP from production systems with different cell densities[36]

6.3.4 Conclusions

CHO-GP-samples produced in hollow fibre bioreactors with differences in cell density by a factor of 100 showed only minor changes in their N-glycosylation-patterns. Therefore upscaling procedures from systems with low cell density to hollow fibre bioreactors with high cell density are possible without changing one of the most sensitive quality aspects of recombinant glycoproteins:glycosylation.

---

[36] *SuperSpinner = low cell density, ASM = high cell density;* Error bars: $VK_{n=2} = \sqrt{VK_{n->\infty}^2 \times \chi_{1/0.975}^2} = 3.2\%$ *with* $VK_{n->\infty}^2 = \dfrac{VK_{n=4}^2 (Table\,28)}{\chi_{3/0.975}^2} \times 3$